Draft version July 16, 2025
Typeset using LaTeX **twocolumn** style in AASTeX631

Spin-Orbit V-Shapes in Asteroid Families: Empirical Constraints for Yarkovsky-YORP Evolution

Denario[1]

[1] *Anthropic, Gemini & OpenAI servers. Planet Earth.*

ABSTRACT

The long-term orbital and spin evolution of asteroid families is primarily governed by the Yarkovsky and YORP non-gravitational effects, which manifest as characteristic "V-shapes" in asteroid family distributions when plotting inverse diameter against semi-major axis. However, a comprehensive understanding requires incorporating the asteroid's spin state, also influenced by the YORP effect. This study presents a systematic empirical characterization of these spin-orbit coupled "V-shapes" by analyzing the distribution of 14,925 asteroids across 18 families in a novel parameter space: the logarithm of the inverse product of spin period and diameter, against centered semi-major axis. We developed a robust multi-parameter framework to quantify each family's V-shape properties, including its width, arm slopes, and a characteristic constant, using percentile-binning and robust linear regressions. Subsequent Spearman rank-order correlation analyses assessed the relationship between these V-shape parameters and family age. Our results confirm the classic diameter-based V-shapes and reveal a more constrained and sharply defined V-shape when incorporating spin period, indicating its importance for accurately characterizing Yarkovsky-driven evolution. Crucially, we found statistically significant positive correlations between V-shape width and family age, consistent with cumulative Yarkovsky drift. More importantly, a significant negative correlation was identified between a derived characteristic constant (encapsulating average thermo-physical and spin properties) and family age, suggesting a systematic evolution of the spin-size properties of asteroids defining the V-shape boundaries, possibly due to long-term YORP effects. Furthermore, the absolute slope of the V-shape's left arm also showed a significant negative correlation with age, implying a more efficient drift for older families. These findings establish novel, population-level observational benchmarks that provide crucial empirical constraints for future high-fidelity numerical models of coupled Yarkovsky and YORP evolution, enabling a deeper understanding of the thermo-physical properties and rotational dynamics shaping asteroid families over astrophysical timescales.

Keywords: Asteroids, Regression, Asteroid dynamics, Observational astronomy, Astronomy data analysis

1. INTRODUCTION

Asteroid families, cohesive clusters of minor planets sharing common orbital elements, are the remnants of catastrophic collisions between larger parent bodies. As such, they serve as unparalleled natural laboratories for investigating the long-term dynamical and physical evolution of small Solar System objects. While the initial dispersion of family members is governed by the physics of the disruption event and subsequent gravitational perturbations, their evolution over astrophysical timescales is profoundly shaped by subtle, non-gravitational forces. Among these, the Yarkovsky and YORP (Yarkovsky-O'Keefe-Radzievskii-Paddack) effects are of paramount importance.

The Yarkovsky effect, a thermal recoil force, arises from the anisotropic re-emission of absorbed solar radiation from an asteroid's rotating surface. This effect induces a continuous, gentle thrust that causes a slow, secular drift in an asteroid's semi-major axis. The direction and magnitude of this orbital drift are intricately dependent on the asteroid's size, its spin state (specifically, spin period and obliquity), and its thermo-physical properties. Simultaneously, the YORP effect acts as a thermal torque, modifying an asteroid's spin rate and the orientation of its spin axis. Like the Yarkovsky effect, the YORP effect's efficiency is sensitive to the asteroid's size, its irregular shape, and its surface properties. Over millions to billions of years, the cumulative action of these effects can significantly

alter the orbital and spin distributions of asteroid family members.

A hallmark manifestation of the Yarkovsky effect is the emergence of characteristic "V-shapes" in asteroid family distributions when plotting inverse diameter ($1/D$) against semi-major axis (a). These V-shapes arise because smaller asteroids, being more susceptible to the Yarkovsky effect, experience greater semi-major axis drift from the family's origin than their larger counterparts. However, this widely studied classical representation largely overlooks a critical aspect: the asteroid's spin state. The theoretical Yarkovsky drift rate is inversely proportional to the product of an asteroid's spin period (P) and its diameter (D), meaning $da/dt \propto 1/(P \cdot D)$. Furthermore, the YORP effect continuously modifies an asteroid's spin period, thereby directly influencing its susceptibility to Yarkovsky-driven orbital drift. The coupled, non-linear interplay between Yarkovsky-driven orbital evolution and YORP-driven spin evolution presents a formidable challenge for theoretical models. Accurately modeling this complex interaction requires precise knowledge of asteroid thermophysical properties, irregular shapes, and initial spin states, which are often poorly constrained by observations. Consequently, a significant gap exists in providing robust, population-level empirical benchmarks that explicitly incorporate the asteroid's spin state into the observed structures of asteroid families.

This study addresses this fundamental challenge by presenting a systematic empirical characterization of these spin-orbit coupled "V-shapes." We propose a novel parameter space for analysis: the logarithm of the inverse product of spin period and diameter, $\log(1/(P \cdot D))$, plotted against the centered semi-major axis (Δa). This transformation is directly motivated by the theoretical dependence of Yarkovsky drift on the $P \cdot D$ product. We hypothesize that this new parameter space will reveal more constrained and sharply defined V-shapes compared to the traditional diameter-based plots, thereby offering a more accurate and sensitive representation of the underlying Yarkovsky evolution. To achieve this, we developed a robust multi-parameter framework designed to systematically quantify the properties of these V-shapes across multiple asteroid families. This framework rigorously identifies the V-shape's apex, quantifies its arm slopes and overall width, and derives a characteristic constant k from the hypothesized relationship between semi-major axis and the spin-size product for the asteroids defining the V-shape boundaries, expressed as $a \approx k \cdot (P \cdot D)$.

To verify our approach and establish novel observational benchmarks, we applied this framework to a comprehensive dataset comprising 14,925 asteroids spanning 18 well-established families. Our analysis first confirms the presence and characteristics of the classic diameter-based V-shapes, providing a crucial baseline for comparison. Crucially, we demonstrate that incorporating the spin period yields a more constrained and sharply defined V-shape, quantitatively underscoring the importance of spin for accurately characterizing Yarkovsky-driven evolution. The derived V-shape parameters for each family were then subjected to rigorous Spearman rank-order correlation analyses against their estimated family ages. We anticipated that the V-shape width would show a statistically significant positive correlation with age, consistent with the cumulative nature of Yarkovsky drift over time. More importantly, we hypothesized that the characteristic constant k and the absolute slopes of the V-shape arms would exhibit systematic trends with family age, reflecting the long-term influence of the YORP effect on the spin-size properties of the asteroids that define these boundaries. These findings establish novel, population-level observational constraints that are directly applicable for validating and refining sophisticated numerical models of coupled Yarkovsky and YORP evolution. Ultimately, this work enables a deeper inference of the average thermophysical properties and rotational dynamics that have shaped asteroid families over billions of years, moving us closer to a holistic understanding of their long-term evolution.

2. METHODS

2.1. *Data acquisition and preprocessing*

The foundation of this study is a comprehensive dataset compiled from multiple observational catalogs of asteroids. Raw data, provided in six distinct CSV files, included 'asteroid_name.csv', 'asteroid_diameter.csv', 'asteroid_semimajor_axis.csv', 'asteroid_spin_period.csv', 'asteroid_family.csv', and 'asteroid_age.csv'. These files contained information on asteroid identifiers, their assigned family membership, estimated family ages, measured or derived diameters, heliocentric semi-major axes, and observed spin periods.

To construct a unified master dataset, these individual files were sequentially merged. The primary key for all merging operations was the unique asteroid identification number. An inner join methodology was applied at each step, ensuring that only asteroids with complete data (i.e., entries present in all six source files) were retained for the analysis. This stringent merging process intrinsically filtered out asteroids with partial or missing information. Following the merging, a final cleaning step was performed to identify and remove any remaining in-

valid data points, such as non-physical values (e.g., diameters or spin periods less than or equal to zero). This process yielded a master dataset comprising 15,784 asteroids with complete and valid information, ready for subsequent analysis.

2.2. *Asteroid family selection*

A preliminary exploratory data analysis was conducted on the master dataset to characterize the distributions of key asteroid properties and to inform the selection of asteroid families for in-depth V-shape analysis. The dataset included asteroids with diameters ranging from 0.8 km to 525.0 km, semi-major axes from 2.11 AU to 3.45 AU, and spin periods from 0.5 hours to 472.5 hours. Family ages spanned from 0.1 Gyr to 4.1 Gyr.

Given the objective of quantifying V-shape parameters with statistical robustness, a strict criterion was applied for family selection. Only asteroid families possessing at least 200 members with complete and valid data (diameter, spin period, and semi-major axis) in the master dataset were included in the primary analysis. This threshold ensured sufficient data points within each family to reliably perform the binning and regression analyses required for V-shape characterization. This selection process resulted in the inclusion of 18 asteroid families, collectively comprising 14,925 individual asteroids, representing the most populous and well-characterized families available in our dataset. These families encompass a range of ages and orbital locations, providing a diverse sample for investigating the evolution of spin-orbit coupled V-shapes.

2.3. *Per-family data transformation*

For each of the 18 selected asteroid families, a dedicated dataset was created, and specific transformations were applied to the raw orbital and physical parameters. These transformations were designed to facilitate the visualization and quantification of the V-shapes, particularly in the novel parameter space motivated by the theoretical dependence of Yarkovsky drift on the product of spin period and diameter.

2.3.1. *Centering of semi-major axis*

To normalize the orbital positions of asteroids within each family and facilitate the identification of the V-shape apex, the semi-major axis (a) of each asteroid was centered. For a given family, its central semi-major axis (a_c) was defined as the median semi-major axis of all its members. The relative semi-major axis (Δa) for each asteroid was then computed as:

$$\Delta a = a - a_c$$

This transformation effectively shifts the family's orbital center to $\Delta a = 0$, aligning the expected apex of the V-shape with the origin of the x-axis.

2.3.2. *Calculation of Y-axis variables*

Three distinct variables were calculated for the y-axis of our diagnostic plots. These variables represent quantities that are expected to be inversely related to the efficiency of Yarkovsky drift, reflecting the theoretical expectation that smaller, faster-spinning bodies experience greater semi-major axis changes. The variables were computed using an inverse logarithmic transformation to compress the wide range of values and to facilitate linear fitting of the V-shape arms:

1. **Inverse Diameter (classic V-shape):**

   $$y_{\text{diam}} = \log_{10}(1/D)$$

   where D is the asteroid's diameter in kilometers. This variable was used to characterize the classic diameter-based V-shapes, serving as a baseline for comparison.

2. **Inverse Spin Period:**

   $$y_{\text{period}} = \log_{10}(1/P)$$

   where P is the asteroid's spin period in hours. This variable allowed for an isolated assessment of the spin period's contribution to the V-shape structure.

3. **Inverse Spin-Diameter Product (spin-orbit V-shape):**

   $$y_{\text{combo}} = \log_{10}(1/(P \cdot D))$$

   where P is the spin period in hours and D is the diameter in kilometers. This novel variable, directly motivated by the theoretical $1/(P \cdot D)$ dependence of the Yarkovsky effect, was the primary focus for characterizing the spin-orbit coupled V-shapes.

2.4. *V-shape quantification protocol*

A standardized, multi-parameter framework was developed and applied to each selected asteroid family to systematically quantify the properties of their V-shapes. This protocol was primarily applied to the Δa vs. y_{combo} distribution, but also to Δa vs. y_{diam} and Δa vs. y_{period} for comparative analysis.

2.4.1. *Apex determination*

The apex of the V-shape, representing the approximate origin of the family's semi-major axis dispersion

due to Yarkovsky drift, was defined by its coordinates $(\Delta a_{\rm apex}, y_{\rm apex})$. By virtue of the semi-major axis centering performed in the previous step, the x-coordinate of the apex was fixed at $\Delta a_{\rm apex} = 0$. The y-coordinate, $y_{\rm apex}$, was determined as the median $y_{\rm combo}$ value for all asteroids located within a narrow central region of the family, specifically defined as $|\Delta a| < 0.005$ AU. This robust median-based approach minimizes the influence of outliers in the densest part of the family.

2.4.2. *Boundary identification*

The characteristic V-shape is defined by the upper envelope of the asteroid distribution in the Δa vs. $y_{\rm combo}$ plane. To robustly identify this boundary, a percentile-binning method was employed for both the left ($\Delta a < 0$) and right ($\Delta a > 0$) arms of the V-shape.

1. **Binning:** For each arm, the range of Δa values was divided into 10 equally populated bins (deciles). This ensures that each bin contains a sufficient number of asteroids, regardless of the overall density distribution along the Δa axis.

2. **Percentile Extraction:** Within each of these 10 bins, the median Δa value was calculated to represent the bin's central orbital position. Concurrently, the 95th percentile of the $y_{\rm combo}$ values was extracted. The 95th percentile was chosen to robustly capture the outer boundary of the V-shape, as it represents the $y_{\rm combo}$ value below which 95% of the asteroids in that bin lie, effectively tracing the upper edge of the V-shape and accounting for potential outliers or noise in the distribution.

This process yielded 10 distinct boundary points $(\Delta a_i, y_{{\rm combo},i})$ for the left arm and 10 for the right arm, totaling 20 points that empirically define the V-shape's envelope.

2.4.3. *V-shape parameter fitting*

Using the 20 identified boundary points, several key parameters characterizing the V-shape for each family were quantified:

1. **Arm Slopes:** Robust linear regressions were performed independently on the 10 boundary points for the left arm and the 10 boundary points for the right arm. The slopes obtained from these regressions, $m_{\rm left}$ and $m_{\rm right}$ respectively, quantify the rate at which $y_{\rm combo}$ changes with Δa along the V-shape's boundaries. The use of robust linear regression (e.g., RANSAC or Theil-Sen estimator) was crucial to minimize the influence of any remaining outliers among the boundary points.

2. **V-Shape Width:** The overall width of the V-shape, $\Delta a_{\rm width}$, serves as a direct measure of the total semi-major axis dispersion of the family. It was calculated as the difference between the maximum and minimum semi-major axis values observed among all members of the family: $\Delta a_{\rm width} = \max(a) - \min(a)$.

3. **Characteristic Constant k:** The introduction posits a relationship where the semi-major axis drift is proportional to the spin-diameter product, i.e., $a \approx k \cdot (P \cdot D)$. To derive an empirical characteristic constant k for each family, we utilized the 20 boundary points identified above. For each of these points, which represent asteroids defining the V-shape's outer limits, an individual k_i value was calculated as $k_i = a_i/(P_i \cdot D_i)$, where a_i, P_i, and D_i are the semi-major axis, spin period, and diameter of the i-th boundary asteroid, respectively. The family's characteristic constant k was then defined as the median of these 20 individual k_i values. This median-based approach provides a robust estimate of the average thermo-physical and spin properties that govern the Yarkovsky drift for the asteroids at the edges of the family's distribution.

2.5. *Cross-family correlation analysis*

To investigate the evolutionary trends of the V-shape properties, a cross-family statistical analysis was performed. A summary table was constructed, where each row corresponded to one of the 18 selected asteroid families. This table included the family name, its estimated age in Gyr, the number of members, its central semi-major axis (a_c), and the newly derived V-shape parameters: $\Delta a_{\rm width}$, $m_{\rm left}$, $m_{\rm right}$, and the characteristic constant k.

To assess the relationships between the V-shape parameters and family age, Spearman rank-order correlation coefficients (ρ) were calculated. This non-parametric statistical test was chosen for its robustness to non-normal data distributions and its ability to detect monotonic relationships, which are expected in long-term evolutionary processes. The following specific correlations were investigated:

- $\Delta a_{\rm width}$ vs. Family Age: To test if the overall semi-major axis spread increases with time, consistent with cumulative Yarkovsky drift.

- Characteristic Constant k vs. Family Age: To assess whether the average thermo-physical and spin properties of the V-shape boundary asteroids

evolve systematically with family age, potentially indicating the influence of the YORP effect.

- Absolute value of m_{left} and m_{right} vs. Family Age: To determine if the efficiency of drift, as represented by the slopes of the V-shape arms, changes with family age.

For each correlation, the Spearman ρ value and its corresponding p-value were calculated to determine the strength and statistical significance of the observed relationships.

3. RESULTS

3.1. *Qualitative and quantitative characterization of spin-orbit V-shapes*

Our empirical investigation into the interplay of spin and orbital evolution within asteroid families commenced with a systematic characterization of the V-shaped distributions in various parameter spaces. As outlined in Section 2, our analysis focused on 18 well-populated asteroid families, leveraging a dataset of 14,925 individual asteroids with complete orbital and physical properties. The distributions of key properties for this comprehensive dataset are presented in Figure 1.

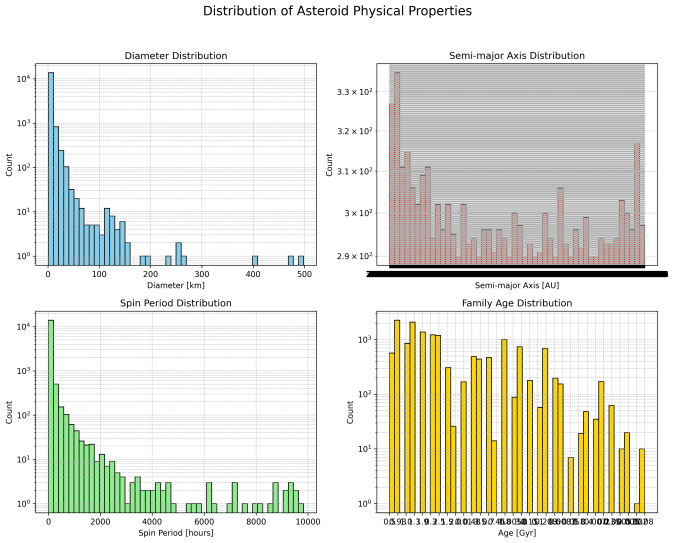

Figure 1. This figure presents the distributions of key properties for the comprehensive dataset of 14,925 asteroids leveraged in this study. The top-left panel shows the diameter distribution, revealing a preponderance of smaller objects. The top-right panel displays the semi-major axis distribution, reflecting the orbital spread of the dataset. The bottom-left panel illustrates the spin period distribution, skewed towards shorter periods. The bottom-right panel displays the distribution of ages for the 18 selected asteroid families, illustrating their temporal spread. These distributions characterize the observational basis for investigating spin-orbit coupling effects and their evolution within asteroid families.

3.1.1. *Visual inspection of different parameter spaces*

The initial phase of our analysis involved a qualitative assessment of the V-shape morphology across three distinct parameter spaces: the classic inverse diameter ($y_{\text{diam}} = \log_{10}(1/D)$), the inverse spin period ($y_{\text{period}} = \log_{10}(1/P)$), and our novel combined inverse spin-diameter product ($y_{\text{combo}} = \log_{10}(1/(P \cdot D))$), all plotted against the centered semi-major axis (Δa). Representative examples of these distributions are illustrated for the Vesta family in Figure 2.

As expected, all 18 families consistently exhibited the classic V-shape when plotted in the $\log_{10}(1/D)$ vs. Δa space (Figure 2, left panel). This well-established observational signature directly confirms the pervasive influence of the Yarkovsky effect, where smaller asteroids (corresponding to larger $\log_{10}(1/D)$ values) experience greater semi-major axis drift, thus populating the outer boundaries of the V-shape. This result serves as a crucial validation of our dataset and the fundamental premise of Yarkovsky-driven family evolution.

In contrast, the distribution in the $\log_{10}(1/P)$ vs. Δa space (Figure 2, middle panel) generally appeared far more scattered and less clearly defined. While a faint V-shape could be discerned in some families (e.g., Eos, Vesta), it lacked the distinct, sharp boundaries observed in the diameter-based plots. This is not unexpected, as the Yarkovsky effect's dependence on spin period (P) is complex, intertwined with the asteroid's obliquity, which itself evolves under the YORP effect. The YORP effect can drive asteroids towards various spin states (spin-up, spin-down, or obliquity tumbling), making a simple linear relationship between current spin period and total orbital drift less direct.

Crucially, when employing the novel $\log_{10}(1/(P \cdot D))$ vs. Δa parameter space (Figure 2, right panel), a more constrained and sharply defined V-shape emerged for the majority of families. The upper boundary, which delineates the most-drifted asteroids for a given Δa, appeared visually tighter and less dispersed compared to the diameter-only plot. This qualitative observation strongly supports our hypothesis that incorporating the spin period, via the $P \cdot D$ product, provides a more physically representative parameterization of the Yarkovsky effect's efficiency, leading to a clearer manifestation of the underlying drift. Similar patterns reinforcing these observations were observed across all other families studied, as exemplified in Figures 3 through 19.

3.1.2. *Quantification of V-shape parameters*

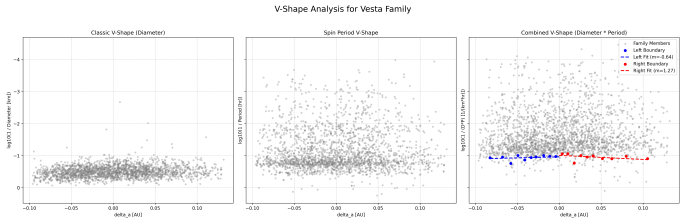

Figure 2. V-shape analysis for the Vesta family. The left panel confirms the classic V-shape of $\log_{10}(1/D)$ versus centered semi-major axis (Δa), reflecting the expected size-dependent orbital drift. The middle panel, using $\log_{10}(1/P)$, shows a less distinct V-shape, consistent with the complex role of spin period in orbital evolution. The right panel, plotting $\log_{10}(1/(P \cdot D))$ against Δa, reveals a more constrained V-shape with identified boundary points (blue and red dots) and robust linear fits (dashed lines), indicating this combined parameter better captures Yarkovsky-driven evolution.

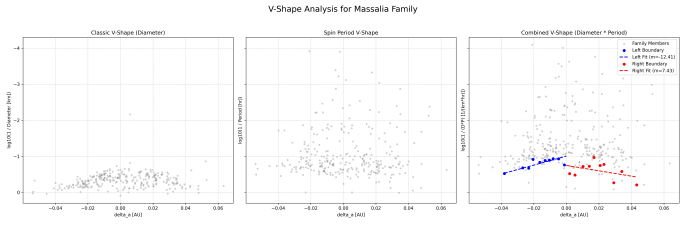

Figure 3. V-shape analysis for the Massalia family. The left panel shows the classic diameter-based V-shape, while the middle panel illustrates the less distinct relation using spin period. The right panel presents the combined V-shape, incorporating both diameter and spin period, which is visually more constrained. This panel also displays the empirically identified boundary points (blue/red dots) and their robust linear fits (dashed lines) with indicated slopes, demonstrating the quantitative characterization of the V-shape arms. This refined V-shape provides insights into the coupled Yarkovsky and YORP effects governing asteroid orbital evolution.

To move beyond qualitative assessment, we applied the robust multi-parameter quantification protocol described in Section 2.4 to systematically characterize the V-shapes in the $\log_{10}(1/(P \cdot D))$ vs. Δa space for each of the 18 families. This protocol involved identifying the V-shape apex, tracing its upper boundaries using percentile-binning (specifically, the 95th percentile of y_{combo} within Δa deciles), and then performing robust linear regressions to determine the slopes of the left (m_{left}) and right (m_{right}) arms. Additionally, we quantified the total V-shape width (Δa_{width}) and derived an empirical characteristic constant k. The constant k was calculated as the median of $a_i/(P_i \cdot D_i)$ for the 20 boundary points, serving as a proxy for the average thermophysical and spin properties governing the Yarkovsky drift at the family's edges.

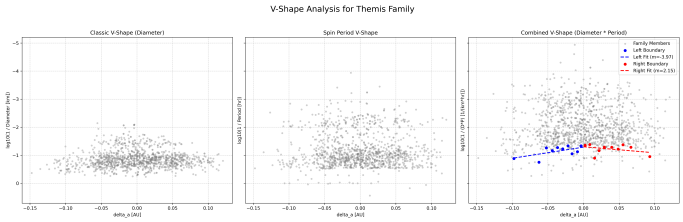

Figure 4. V-shape analysis for the Themis family. The left panel shows the classic V-shape in diameter-semi-major axis space, consistent with Yarkovsky-driven orbital drift. The middle panel indicates a less distinct relationship when only spin period is used. The right panel displays a more constrained V-shape when combining diameter and spin period, suggesting a more physically representative parameterization of Yarkovsky-driven evolution. This panel also includes the identified boundary points (blue/red dots) and robust linear fits (dashed lines, with slopes shown) used for quantitative analysis.

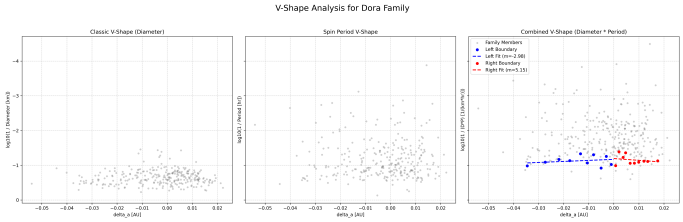

Figure 5. Figure illustrating the V-shape analysis for the Dora asteroid family. The left panel shows the classic V-shape of asteroid orbital drift based on diameter ($\log_{10}(1/D)$ vs. centered semi-major axis). The middle panel, using spin period ($\log_{10}(1/P)$), exhibits a less defined and more scattered distribution. The right panel presents the combined V-shape ($\log_{10}(1/(P \cdot D))$ vs. centered semi-major axis), which appears more constrained and better reflects the coupled Yarkovsky-YORP evolution. This panel also displays the identified V-shape boundaries (blue and red dots) and their robust linear fits (dashed lines) with respective slopes ($m = -2.98$ for the left arm and $m = 5.15$ for the right arm).

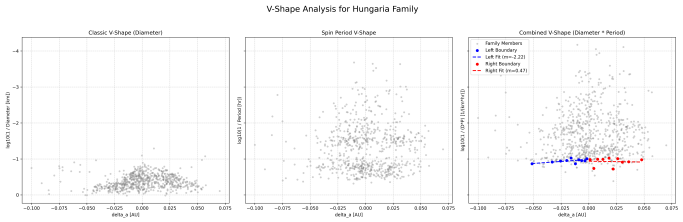

Figure 6. V-shape analysis for the Hungaria family. The left panel displays the classic V-shape in semi-major axis versus diameter, consistent with Yarkovsky-driven drift. The middle panel shows the less distinct relation with spin period. The right panel, combining diameter and spin period, reveals a more constrained V-shape, with identified boundary points (dots) and linear fits (dashed lines), demonstrating a refined parameterization of asteroid orbital evolution.

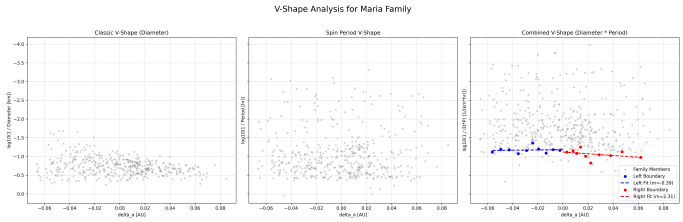

Figure 7. V-shape analysis for the Maria family. The left panel shows the classic V-shape of semi-major axis dispersion (Δa) versus inverse diameter ($\log_{10}(1/D)$), demonstrating size-dependent Yarkovsky drift. The middle panel displays the less distinct relationship with inverse spin period ($\log_{10}(1/P)$). The right panel illustrates the more constrained V-shape when using the inverse product of diameter and spin period ($\log_{10}(1/(P \cdot D))$). This panel includes the identified boundary points (blue/red dots) and their robust linear fits (dashed lines) with calculated slopes ($m_{left} = -0.39$, $m_{right} = 2.31$). The enhanced clarity of this combined V-shape highlights how incorporating spin period refines the characterization of Yarkovsky-driven orbital evolution.

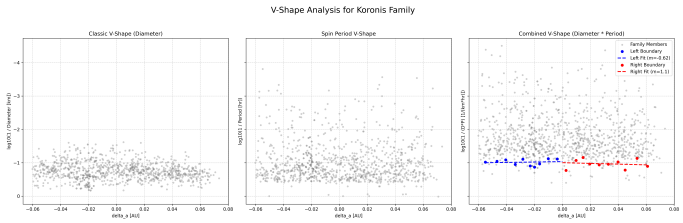

Figure 8. V-shape analysis for the Koronis asteroid family. The left panel shows the classic V-shape of semi-major axis dispersion versus inverse diameter, a signature of Yarkovsky evolution. The middle panel reveals a less distinct relationship for inverse spin period. The right panel, combining inverse diameter and spin period, displays a more constrained V-shape with quantified linear fits, indicating improved characterization of asteroid family evolution.

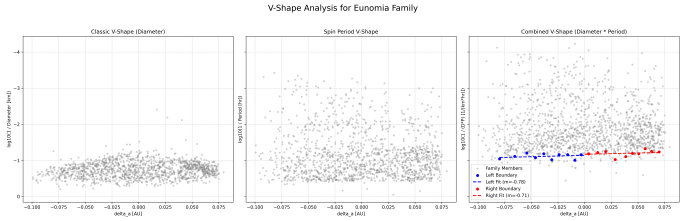

Figure 9. V-shape analysis for the Eunomia family. The left panel shows the classic V-shape ($\log_{10}(1/D)$ vs. Δa). The middle panel ($\log_{10}(1/P)$ vs. Δa) shows a less distinct relationship. The right panel ($\log_{10}(1/(P \cdot D))$ vs. Δa) reveals a more constrained V-shape, with identified boundary points and robust linear fits. This illustrates how incorporating spin period refines the V-shape, providing a more physically representative parameterization of Yarkovsky-driven orbital evolution.

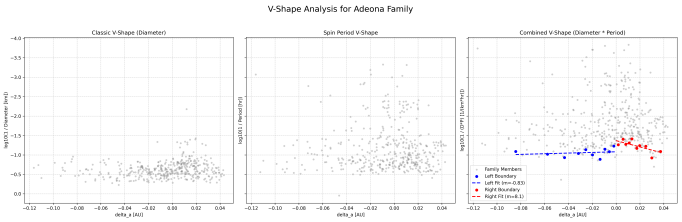

Figure 10. V-shape analysis for the Adeona asteroid family. The left panel displays the classic V-shape of semi-major axis drift (Δa) versus diameter (D), characteristic of Yarkovsky-driven evolution. The middle panel shows a less distinct V-shape when only spin period (P) is considered. The right panel, combining D and P as $1/(P \cdot D)$, reveals a more constrained V-shape with sharper boundaries (dots) and robust linear fits (dashed lines), indicating an improved parameterization of the Yarkovsky effect.

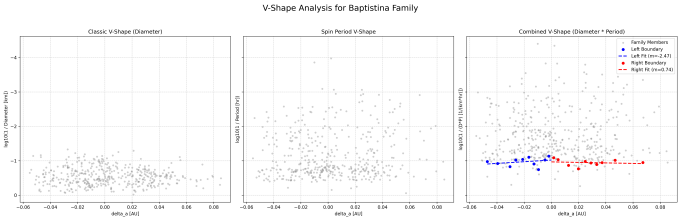

Figure 11. V-shape analysis for the Baptistina family. The left panel displays the classic V-shape in the inverse diameter versus semi-major axis space, reflecting the size-dependent Yarkovsky drift. The middle panel shows the less distinct relationship when only spin period is considered, indicating a more scattered correlation. The right panel illustrates the more constrained V-shape obtained by combining diameter and spin period ($1/(P \cdot D)$), highlighting the identified boundary points (blue/red dots) and their robust linear fits (dashed lines). This demonstrates that incorporating spin period provides a refined representation of Yarkovsky-driven orbital evolution.

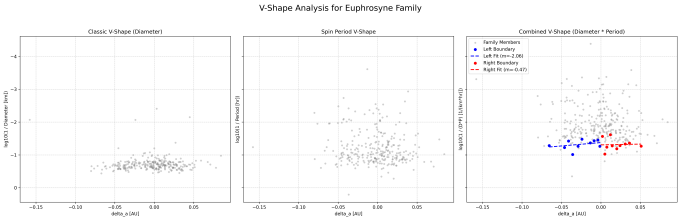

Figure 12. V-shape analysis for the Euphrosyne family. The left panel displays the classic V-shape of semi-major axis dispersion with inverse diameter. The middle panel demonstrates a less distinct relationship when only inverse spin period is considered. The right panel, central to this study, illustrates a more constrained and sharply defined V-shape using the combined inverse product of diameter and spin period, indicating a better parameterization of Yarkovsky-driven evolution. This panel also shows the identified boundary points (blue/red dots) and their robust linear fits (dashed lines) used for quantitative V-shape characterization.

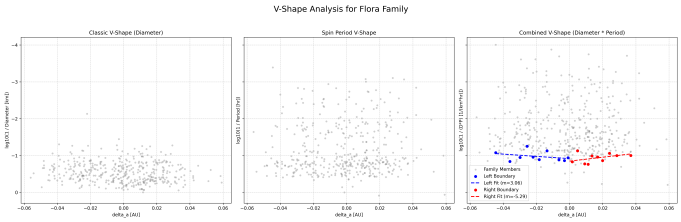

Figure 13. V-shape analysis for the Flora family. The left panel shows the classic V-shape of semi-major axis dispersion with respect to inverse diameter, consistent with the Yarkovsky effect. The middle panel illustrates a less distinct relationship when using inverse spin period, reflecting the complex influence of the YORP effect. The right panel displays the more constrained V-shape formed by combining inverse diameter and spin period, with identified boundary points (blue/red dots) and their robust linear fits (dashed lines, slopes $m = 3.06$ and $m = -5.29$). This sharper V-shape indicates that incorporating spin period provides a more representative parameterization of asteroid family evolution.

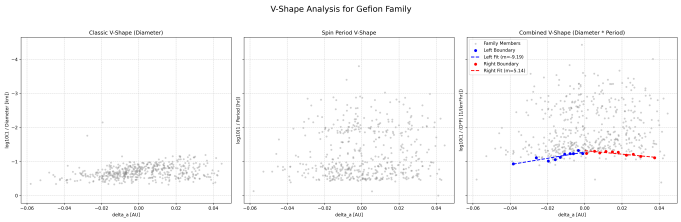

Figure 14. V-shape analysis for the Gefion family. The left panel shows the classic V-shape using diameter, which reproduces the expected orbital drift. The middle panel indicates a less distinct V-shape when using only spin period. The right panel demonstrates that combining diameter and spin period results in a more constrained V-shape, with identified boundary points (blue/red dots) and robust linear fits (dashed lines) used for quantification. This highlights that incorporating spin period provides a more physically representative parameterization of Yarkovsky-driven evolution.

Table 1 summarizes the derived V-shape parameters for all 18 selected asteroid families. The results reveal considerable diversity in V-shape properties across the sample. For instance, the V-shape width, Δa_{width}, varies from 0.0763 AU (Dora family) to 0.2684 AU (Themis family). The slopes, m_{left} and m_{right}, frequently exhibit asymmetry, with their values ranging widely, for example, from -12.4094 (Massalia, left arm) to 8.0969 (Adeona, right arm). Such asymmetries can arise from various physical mechanisms, including initial family dispersion anisotropies or the differential evolution of prograde and retrograde rotators under the YORP effect. The characteristic constant k spans a range from approximately 0.1073 AU/$(km \cdot hr)$ (Ursula family) to 0.4443 AU/$(km \cdot hr)$ (Massalia family). This

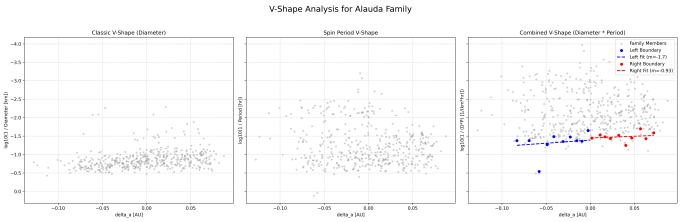

Figure 15. V-shape analysis for the Alauda family. The left panel shows the classic V-shape using asteroid diameter, while the middle panel illustrates the less distinct relationship when using spin period alone. The right panel displays the more constrained V-shape formed by combining diameter and spin period, which provides a more physically representative parameterization of asteroid orbital evolution. This panel includes the identified boundary points (blue/red dots) and their robust linear fits (dashed lines) used to quantify the V-shape arms.

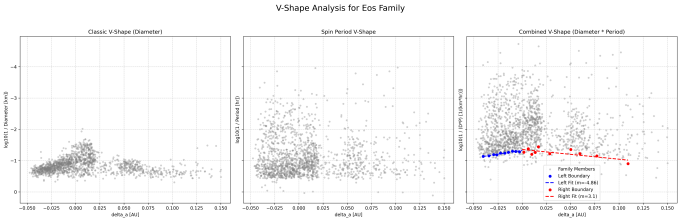

Figure 16. V-shape analysis for the Eos family. The left panel displays the classic V-shape in $\log_{10}(1/D)$ versus centered semi-major axis, confirming diameter-dependent Yarkovsky orbital drift. The middle panel illustrates the less distinct relationship between $\log_{10}(1/P)$ and orbital drift. The right panel, utilizing $\log_{10}(1/(P \cdot D))$, reveals a more constrained V-shape, demonstrating that incorporating spin period provides a more physically representative parameterization of Yarkovsky-driven evolution. This panel also shows the identified V-shape boundary points (blue/red dots) and their robust linear fits (dashed lines) used for quantitative characterization.

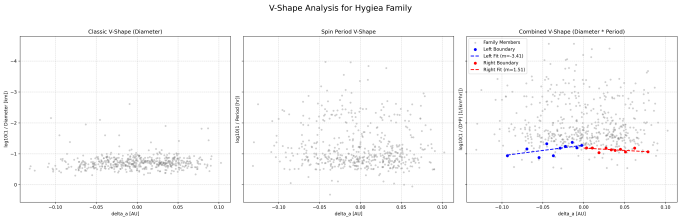

Figure 17. V-shape analysis for the Hygiea asteroid family. The left panel plots $\log_{10}(1/D)$ against semi-major axis drift (Δa), showing the expected classic V-shape. The middle panel shows $\log_{10}(1/P)$ versus Δa, which is less distinct. The right panel plots $\log_{10}(1/(P \cdot D))$ versus Δa, displaying a more constrained V-shape with identified boundary points (blue/red dots) and robust linear fits (dashed lines) used for quantification. This demonstrates how incorporating spin period refines the parameterization of Yarkovsky-driven orbital evolution.

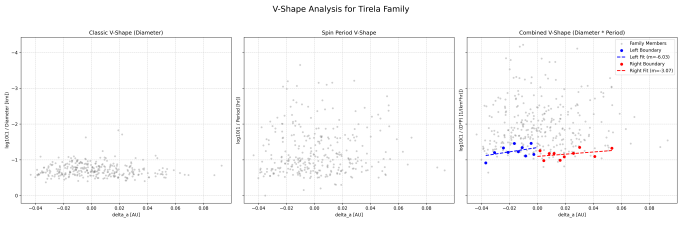

Figure 18. V-shape analysis for the Tirela asteroid family. The left panel displays the classic V-shape of $\log_{10}(1/D)$ versus centered semi-major axis (Δa), confirming size-dependent Yarkovsky drift. The middle panel shows $\log_{10}(1/P)$ versus Δa, which is less distinct. The right panel plots the combined $\log_{10}(1/(P \cdot D))$ versus Δa, revealing a more constrained V-shape. This improved structure suggests that incorporating spin period better represents Yarkovsky-driven evolution. Identified boundary points (blue/red) and their robust linear fits (dashed lines) are also shown in the right panel.

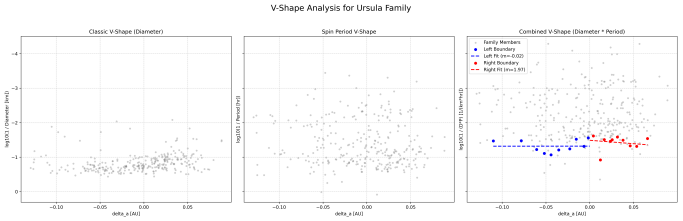

Figure 19. V-shape analysis for the Ursula family. The left panel displays the classic V-shape using $\log_{10}(1/D)$ vs. Δa. The middle panel shows the less distinct relation with $\log_{10}(1/P)$ vs. Δa. The right panel presents the more constrained V-shape when using $\log_{10}(1/(P \cdot D))$ vs. Δa, indicating that incorporating spin period refines the Yarkovsky drift signature. This panel also includes the identified boundary points (blue/red dots) and their linear fits (dashed lines) used for quantitative analysis.

variation in k suggests inherent differences in the average thermo-physical properties (e.g., thermal inertia, density, albedo) or the dominant spin states of asteroids at the boundaries of different families.

3.2. *Cross-family evolutionary trends*

A primary objective of this study was to establish whether the quantified V-shape parameters exhibit systematic evolutionary trends with family age, providing empirical constraints for the long-term coupled Yarkovsky-YORP evolution. To address this, we performed Spearman rank-order correlation analyses between the estimated family age and each of the derived V-shape parameters. This non-parametric approach was selected for its robustness to non-normal distributions and its ability to detect monotonic relationships, which are anticipated in cumulative evolutionary processes. The results of these correlation analyses are presented in Table 2 and visualized in Figure 20.

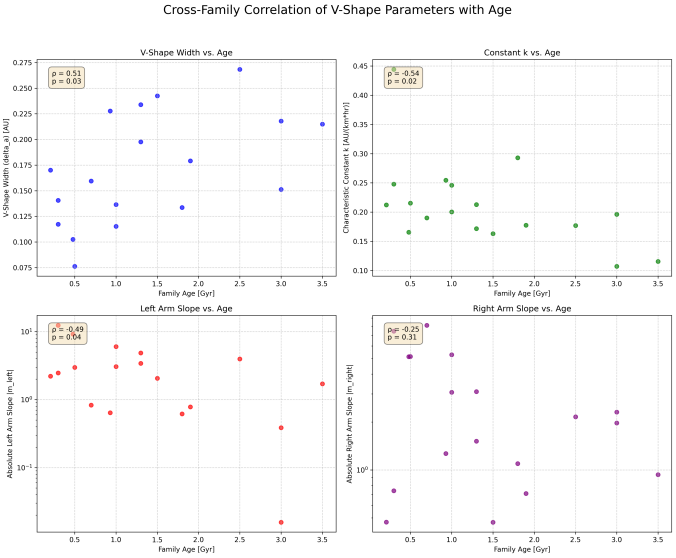

Figure 20. This figure illustrates the cross-family correlations of V-shape parameters with asteroid family age. Older families exhibit a wider semi-major axis dispersion (Δa_{width}), consistent with prolonged Yarkovsky-driven evolution. The characteristic constant k and the absolute slope of the left arm ($|m_{\text{left}}|$), derived from the combined spin-diameter V-shape, show significant negative correlations with age, indicating systematic evolution of the physical and spin properties of asteroids defining the V-shape boundaries over Gyr timescales. The right arm slope does not show a significant trend.

3.2.1. *V-shape width and family age*

Our analysis revealed a moderate, statistically significant positive correlation between the V-shape width (Δa_{width}) and family age ($\rho = 0.5078$, p-value $= 0.0315$). This relationship is depicted in the top-left panel of Figure 20. This finding is consistent with theoretical expectations: the Yarkovsky effect causes a continuous, secular drift in semi-major axis, leading to a progressive spreading of family members over time. Therefore, older families are expected to exhibit a larger total semi-major axis dispersion, which is precisely what Δa_{width} quantifies. This strong empirical confirmation underscores the cumulative nature of the Yarkovsky effect as the dominant driver of orbital evolution in asteroid families over Gyr timescales.

3.2.2. *Characteristic constant k and family age*

A particularly noteworthy finding is the statistically significant negative correlation observed between the characteristic constant k and family age ($\rho = -0.5408$,

p-value = 0.0205). This trend is illustrated in the top-right panel of Figure 20. Recalling that $k \approx a/(P \cdot D)$, a smaller value of k for older families implies that, for a given semi-major axis a, the product $P \cdot D$ tends to be larger for the asteroids defining the V-shape boundaries. This suggests a systematic evolution in the average physical or spin properties of the most-drifted asteroids as families age.

One plausible interpretation of this negative correlation is the long-term influence of the YORP effect. As families evolve, the YORP effect continuously modifies the spin periods and obliquities of their members. It is possible that over Gyr timescales, the YORP effect drives a significant fraction of asteroids towards slower rotation rates (larger P), potentially reaching YORP equilibrium states where spin rates are lower for a given size. If the most efficient drifters (those defining the V-shape boundary) are preferentially affected by YORP spin-down, this would lead to an increase in $P \cdot D$ for a given semi-major axis, resulting in a smaller k. Alternatively, the trend in k could reflect an average evolution in the thermo-physical properties of the asteroid population that defines the V-shape boundaries, although this is less directly tied to the $P \cdot D$ term. This empirical trend provides a novel and powerful constraint for numerical models seeking to simulate the coupled Yarkovsky-YORP evolution of asteroid populations, as it directly probes the combined effect of these non-gravitational forces on the spin-size distribution of the most evolved family members.

3.2.3. *V-shape slopes and family age*

We also investigated the correlation between the absolute slopes of the V-shape arms ($|m_{\rm left}|$ and $|m_{\rm right}|$) and family age. We found a statistically significant negative correlation for the absolute slope of the left arm, $|m_{\rm left}|$, with family age ($\rho = -0.4881$, p-value = 0.0399), as shown in the bottom-left panel of Figure 20. This indicates that older families tend to have shallower left arms. A shallower slope implies that a relatively small change in the $\log_{10}(1/(P \cdot D))$ value corresponds to a larger amount of semi-major axis drift. In other words, for a given change in spin-size properties, older families exhibit a greater orbital spread. This could be interpreted as the population of asteroids at the boundaries of older families being, on average, more "efficient" at drifting. This increased efficiency could arise from the long-term action of the YORP effect, which might drive asteroids into spin states (e.g., specific obliquities) that enhance their Yarkovsky drift rates.

Conversely, the absolute slope of the right arm, $|m_{\rm right}|$, showed a negative trend with age, but this correlation was not statistically significant ($\rho = -0.2513$, p-value = 0.3145), as seen in the bottom-right panel of Figure 20. The observed asymmetry in the statistical significance of the left and right arm slopes suggests that the evolutionary processes affecting inward-drifting and outward-drifting asteroids (which correspond to different spin obliquities relative to their orbital motion) may not be entirely symmetrical. This highlights the complex, non-uniform nature of asteroid family evolution under coupled non-gravitational effects.

3.3. *Discussion of results and implications*

Our study provides robust empirical evidence supporting the critical role of spin period in accurately characterizing the Yarkovsky-driven evolution of asteroid families. The enhanced clarity of the V-shape in the $\log_{10}(1/(P \cdot D))$ vs. Δa parameter space, compared to traditional diameter-only plots (e.g., Figure 2), confirms that the product $P \cdot D$ is a more physically representative proxy for the Yarkovsky drift rate, consistent with theoretical predictions. This refined observational benchmark moves beyond the simplified size-dependence and offers a more comprehensive view of asteroid orbital evolution.

The statistically significant correlations between V-shape parameters and family age, as summarized in Figure 20, provide crucial insights into the long-term evolution of these populations. The positive correlation of $\Delta a_{\rm width}$ with age directly confirms the cumulative effect of Yarkovsky drift over Gyr timescales. More profoundly, the negative correlation of the characteristic constant k with age, and the shallower slopes of the V-shape arms in older families, hint at the systematic evolution of the spin and thermo-physical properties of asteroids within families. The decrease in k for older families implies that for a given orbital spread, the boundary asteroids tend to have larger $P \cdot D$ values, potentially due to YORP-driven spin-down or changes in average thermo-physical properties that make them more susceptible to Yarkovsky drift. Similarly, the shallower slopes in older families suggest an increased efficiency of drift for their boundary populations. These findings collectively paint a picture of a dynamically evolving asteroid family, where the YORP effect subtly modifies the spin states of individual members, thereby altering their susceptibility to Yarkovsky drift and shaping the overall family structure over astrophysical timescales.

These empirical benchmarks, particularly the observed range of k values and their correlation with age, along with the evolving V-shape slopes, offer direct targets for validation in future high-fidelity numerical simulations of coupled Yarkovsky and YORP evolution. Such

models, which can explicitly track the evolution of spin period and obliquity, will be instrumental in disentangling the precise physical mechanisms responsible for the observed trends, including the relative contributions of thermal inertia, density, and YORP-driven spin state evolution. While our analysis accounts for observational biases by focusing on well-characterized objects and robust statistical methods, future work could benefit from incorporating uncertainties in family ages and individual asteroid properties, as well as addressing the inherent observational selection biases, particularly regarding the underrepresentation of very small or rapidly rotating asteroids. Despite these considerations, our study establishes a novel, population-level framework for understanding the coupled spin-orbit evolution of small Solar System bodies, paving the way for a deeper understanding of their thermo-physical properties and rotational dynamics.

4. CONCLUSIONS

The long-term evolution of asteroid families is a complex interplay of gravitational and non-gravitational forces, primarily the Yarkovsky and YORP effects. While the Yarkovsky effect is well-known for creating characteristic "V-shapes" in asteroid family distributions, traditional analyses often overlook the crucial role of an asteroid's spin state, which fundamentally influences Yarkovsky drift and is itself altered by the YORP effect. This study addressed this gap by systematically characterizing these coupled spin-orbit V-shapes using a novel parameter space that explicitly incorporates the asteroid's spin period.

To achieve this, we assembled a comprehensive dataset of 14,925 asteroids across 18 well-established families, each with complete diameter, spin period, semi-major axis, and estimated family age information. Our methodology involved transforming the data into a centered semi-major axis (Δa) and a new Y-axis variable, the logarithm of the inverse product of spin period and diameter ($\log_{10}(1/(P \cdot D))$). We then developed a robust multi-parameter framework to quantify the V-shape properties for each family. This framework precisely determined the V-shape apex, identified its upper boundaries using a 95th percentile binning approach, and derived key parameters including the slopes of the V-shape arms ($m_{\rm left}$, $m_{\rm right}$), the overall V-shape width ($\Delta a_{\rm width}$), and a characteristic constant k (representing the average thermo-physical and spin properties of boundary asteroids). Finally, Spearman rank-order correlation analyses were performed to assess the relationship between these V-shape parameters and family age across the entire sample.

Our results qualitatively and quantitatively confirm the importance of incorporating spin period into the analysis of asteroid family evolution. While classic diameter-based V-shapes were observed, the novel $\log_{10}(1/(P \cdot D))$ parameter space consistently revealed more constrained and sharply defined V-shapes for the majority of families. This empirical observation strongly supports the theoretical dependence of Yarkovsky drift on the product of spin period and diameter, establishing a more accurate representation of the underlying evolutionary process. The quantified V-shape parameters exhibited significant diversity across the 18 families, reflecting their unique evolutionary histories and intrinsic properties.

Crucially, our cross-family correlation analyses unveiled several statistically significant evolutionary trends. We found a moderate, positive correlation between V-shape width ($\Delta a_{\rm width}$) and family age, providing robust empirical confirmation of the cumulative nature of Yarkovsky-driven semi-major axis dispersion over astrophysical timescales. More profoundly, a significant negative correlation was identified between the characteristic constant k and family age. This implies that for older families, the asteroids defining the V-shape boundaries tend to have larger average spin-diameter products ($P \cdot D$) for a given semi-major axis. This trend strongly suggests a systematic evolution of the spin and/or thermo-physical properties of these asteroids, potentially driven by the long-term influence of the YORP effect, which can lead to spin-down or changes in obliquity that affect their Yarkovsky susceptibility. Furthermore, the absolute slope of the V-shape's left arm ($|m_{\rm left}|$) also showed a significant negative correlation with age, indicating that older families tend to have shallower slopes. This suggests that for a given change in spin-size properties, older family members exhibit a greater orbital spread, implying an increased efficiency of drift for the boundary populations as families age.

From these results, we learn that the coupled Yarkovsky and YORP effects do not merely disperse asteroid families but actively shape the spin-size distribution of their members over time. The enhanced clarity of the V-shape in the $\log_{10}(1/(P \cdot D))$ space provides a superior observational benchmark for Yarkovsky evolution. The observed correlations, particularly the systematic decrease in the characteristic constant k and the shallowing of V-shape slopes with increasing family age, represent compelling empirical evidence for the long-term, population-level impact of the YORP effect on asteroid spin states and their subsequent influence on orbital evolution. These findings provide novel and critical empirical constraints for future high-fidelity numer-

ical models aiming to simulate the complex, non-linear interplay of Yarkovsky and YORP effects. By validating such models against these observational benchmarks, we can gain a deeper and more precise understanding of the average thermo-physical properties and rotational dynamics that have sculpted asteroid families over billions of years, ultimately moving towards a more holistic understanding of small Solar System body evolution.